Role of dystroglycan in limiting contraction-induced injury to the sarcomeric cytoskeleton of mature skeletal muscle

Erik P. Rader[a,b,c,d], Rolf Turk[a,b,c,d], Tobias Willer[a,b,c,d], Daniel Beltrán[a,b,c,d], Kei-ichiro Inamori[a,b,c,d,e], Taylor A. Peterson[a,b,c,d], Jeffrey Engle[a,b,c,d], Sally Prouty[a,b,c,d], Kiichiro Matsumura[f], Fumiaki Saito[f], Mary E. Anderson[a,b,c,d], and Kevin P. Campbell[a,b,c,d,1]

[a]Howard Hughes Medical Institute, The University of Iowa, Iowa City, IA 52242; [b]Department of Molecular Physiology and Biophysics, The University of Iowa, Iowa City, IA 52242; [c]Department of Neurology, The University of Iowa, Iowa City, IA 52242; [d]Department of Internal Medicine, The University of Iowa, Iowa City, IA 52242; [e]Division of Glycopathology, Institute of Molecular Biomembrane and Glycobiology, Tohoku Medical and Pharmaceutical University, Sendai, Miyagi 981-8558, Japan; and [f]Department of Neurology, Teikyo University School of Medicine, Itabashi-ku, Tokoyo 173-8605, Japan

Edited by Eric N. Olson, University of Texas Southwestern Medical Center, Dallas, TX, and approved August 2, 2016 (received for review April 1, 2016)

Dystroglycan (DG) is a highly expressed extracellular matrix receptor that is linked to the cytoskeleton in skeletal muscle. DG is critical for the function of skeletal muscle, and muscle with primary defects in the expression and/or function of DG throughout development has many pathological features and a severe muscular dystrophy phenotype. In addition, reduction in DG at the sarcolemma is a common feature in muscle biopsies from patients with various types of muscular dystrophy. However, the consequence of disrupting DG in mature muscle is not known. Here, we investigated muscles of transgenic mice several months after genetic knockdown of DG at maturity. In our study, an increase in susceptibility to contraction-induced injury was the first pathological feature observed after the levels of DG at the sarcolemma were reduced. The contraction-induced injury was not accompanied by increased necrosis, excitation–contraction uncoupling, or fragility of the sarcolemma. Rather, disruption of the sarcomeric cytoskeleton was evident as reduced passive tension and decreased titin immunostaining. These results reveal a role for DG in maintaining the stability of the sarcomeric cytoskeleton during contraction and provide mechanistic insight into the cause of the reduction in strength that occurs in muscular dystrophy after lengthening contractions.

muscular dystrophy | eccentric contraction | titin | skeletal muscle | dystroglycan

Muscular dystrophies are a heterogenous group of genetic disorders characterized by progressive muscle weakness and wasting (1, 2). Mutations in genes encoding proteins of the dystrophin–glycoprotein complex (DGC) are associated with various muscular dystrophies (3–10). The DGC is a multimeric complex comprising both transmembrane proteins [β-dystroglycan (DG), sarcoglycans (α, β, γ, and δ), and sarcospan] and membrane-associated proteins (α-DG, dystrophin, syntrophin, dystrobrevin, and neuronal nitric oxide synthase). α- and β-DG are produced by posttranslational cleavage of DG, which is encoded by *DAG1* (11). These subunits are central to linking the extracellular matrix to the intracellular cytoskeleton (6, 11). α-DG undergoes posttranslational glycosylation, which is required for its binding to extracellular-matrix proteins, such as laminin, agrin, neurexin, pickachurin, and perlecan, which bear laminin globular domains (11, 12). One such glycosylation modification is mediated by the glycosyltransferase LARGE and requires the presence of the N terminus of α-DG (12, 13), which is truncated during subsequent processing of the protein (12). The C terminus of α-DG is noncovalently associated with β-DG, a protein that is key to DGC function because it associates with α-DG extracellularly and with dystrophin intracellularly (11). Dystrophin, in turn, binds to the cytoskeleton, through an interaction between its N terminus and F-actin (12, 14). The mechanical link provided by DG and the DGC enables the cytoskeleton to impart tension to the extracellular matrix (15).

Many muscular dystrophies are associated with reduced, but detectable, sarcolemmal immunofluorescence staining of glycosylated α-DG or core α- and β-DG. The extracellular matrix receptor function of α-DG is impaired when either *DAG1* is itself mutated (limb-girdle muscular dystrophy type 2P) (10, 16, 17) or genes that encode putative or known glycosyltransferases that act on α-DG are mutated (Walker–Warburg syndrome, muscle–eye–brain disease, Fukuyama congenital muscular dystrophy, congenital muscular dystrophy types 1C and 1D, or limb-girdle muscular dystrophy) (12, 18, 19). Sarcolemmal expression of α-DG, sarcospan, and the sarcoglycan complex is reduced in patients with distinct sarcoglycan mutations (limb-girdle muscular dystrophy type 2C-F) (3–5, 20). Levels of α-DG, β-DG, the sarcoglycan complex, and sarcospan are reduced at the sarcolemma of patients with dystrophin mutations (Duchenne and Becker muscular dystrophy) (6–9).

Defects in the DGC are associated with high susceptibility to severe muscle injury caused by lengthening contractions (21–24). Muscles of mice deficient for dystrophin (*mdx* mice) display increased sarcolemmal damage, destabilization of sarcomeres, hypercontraction, and contraction-induced force deficits (22, 25–27). Muscles of mice that either lack DG or have mutations that render α-DG hypoglycosylated are significantly more susceptible to severe contraction-induced injury than those of WT counterparts (21).

Significance

Dystroglycan (DG) is an extracellular matrix receptor that is linked to the cytoskeleton and critical for the development of skeletal muscle. DG deficiency throughout development is associated with multiple pathological features and muscular dystrophy. However, the direct consequence of DG disruption in mature muscle is not known. Here, we investigate muscles of transgenic mice after genetic knockdown of DG at maturity. The results demonstrate early susceptibility to contraction-induced injury accompanied by reduced passive tension and decreased titin immunostaining, rather than increased necrosis, excitation–contraction uncoupling, or sarcolemmal fragility. These results suggest a need for critical rethinking of both current theories regarding contraction-induced injury in muscular dystrophy and therapeutic strategies.

Author contributions: E.P.R., R.T., T.W., and K.P.C. designed research; E.P.R., D.B., K.-i.I., T.A.P., J.E., S.P., K.M., F.S., and M.E.A. performed research; E.P.R., R.T., D.B., K.-i.I., M.E.A., and K.P.C. analyzed data; and E.P.R. wrote the paper.

The authors declare no conflict of interest.

This article is a PNAS Direct Submission.

Freely available online through the PNAS open access option.

[1]To whom correspondence should be addressed. Email: kevin-campbell@uiowa.edu.

This article contains supporting information online at www.pnas.org/lookup/suppl/doi:10.1073/pnas.1605265113/-/DCSupplemental.

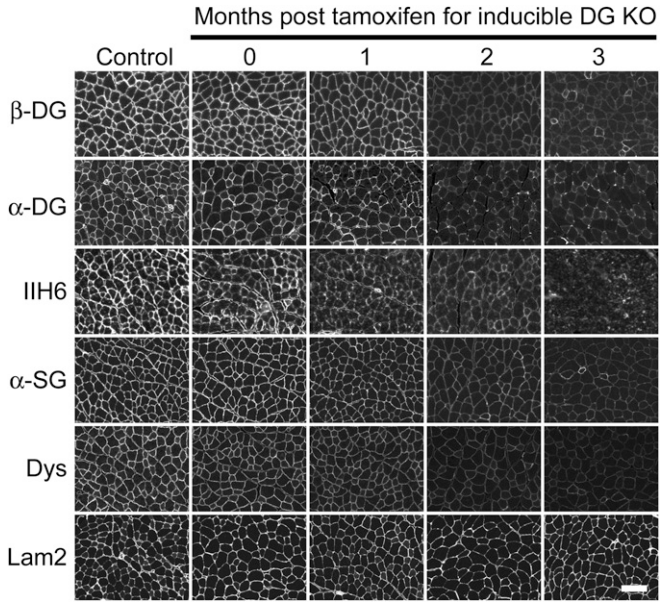

Fig. 1. Upon tamoxifen exposure in skeletal muscle of inducible DG KO mice, DG expression is progressively reduced. Time-dependent reductions in sarcolemma immunostaining were observed for core α-DG, glyco-α-DG (IIH6), and the C terminus of β-DG. A reduction in staining was also observed for α-sarcoglycan (α-SG) and dystrophin (Dys), which are also DGC components. This reduction was not the case for laminin α2 (Lam2). Values are means ± SE. (Scale bar: 100 μm.)

These findings are consistent with the proposal that severe contraction-induced injury exacerbates the dystrophic condition.

Previous research regarding the association of DG function with contraction-induced injury was based on studies in which DG was defective throughout development (21). These analyses failed to distinguish whether increased susceptibility to contraction-induced injury is a direct consequence of DG disruption or an indirect consequence of abnormal development and growth. Here, we find that, in an inducible DG knockout (inducible DG KO) mouse model, susceptibility to injury from lengthening contractions is increased at maturity and in the absence of overt necrosis, which implies that this form of injury is a direct consequence of disruption of the DGC. Interestingly, lengthening contractions reduce immunostaining levels of titin whereas membrane permeability and excitation–contraction uncoupling seem to be unaffected. Overall, these findings contribute to the current theory regarding the mechanism of contraction-induced injury in the dystrophic condition by characterizing the sensitivity of the sarcomeric cytoskeleton to reductions in DG, and the DGC more generally, at maturity.

Results

Induction of *Dag1* Disruption by Tamoxifen Gradually Decreases DG Levels. The effectiveness of tamoxifen in rapidly inducing recombination and decreasing levels of the *Dag1* mRNA in inducible DG KO mice was confirmed by RT-PCR (Fig. S1). A reduction in sarcolemmal staining for core α-DG, glycosylated α-DG, and β-DG was evident by 2 mo after tamoxifen exposure (Fig. 1). A comparable pattern of reduction was observed for the DGC proteins α-sarcoglycan and dystrophin whereas expression of the extracellular laminin α2 protein remained unchanged (Fig. 1). By 2–3 mo after tamoxifen exposure, levels of the DG protein decreased by ∼80%, as assessed by immunoblotting with antibodies for core α-DG, glycosylated α-DG, and β-DG (Fig. S2). Thus, the combination of immunofluorescence staining and Western blotting demonstrates that this inducible mouse model leads to a dramatic knockdown of DG expression at both the mRNA and protein levels after 3 mo, but clearly the mice are not null for DG protein.

Susceptibility to Contraction-Induced Force Deficits Precedes Overt Necrosis. Despite the fact that DG levels were reduced by 3 mo after tamoxifen exposure, no overt necrosis was observed at that time (Fig. S3). Moreover, the percentage of centrally nucleated fibers (0.5 ± 0.3%, n = 5) and variability in muscle fiber area (coefficient of variance = 440 ± 47, n = 5) for inducible DG KO mice did not differ significantly from values for control mice (0.6 ± 0.3% and 478 ± 20 coefficient of variance, n = 5). However, necrosis became apparent later, at 6 mo post-tamoxifen, at which point both the number of centrally nucleated fibers (20.3 ± 4.5%, n = 7) and the coefficient of variance for muscle fiber area (604 ± 42, n = 7) were elevated relative to control values (1.1 ± 0.7% and 486 ± 20, respectively, n = 7, $P < 0.05$). To evaluate muscle function before the onset of overt necrosis, specific force and contraction-induced force deficits were evaluated for muscle ex vivo up to 3 mo after tamoxifen exposure (Fig. 2 and Table S1). At 1 and 2 mo post-tamoxifen exposure, the specific forces in muscles of inducible DG KO mice (237 ± 8 kN/m^2 at 1 mo and 239 ± 5 kN/m^2 at 2 mo, n = 5–8 per group) did not differ significantly from those in controls (243 ± 4 kN/m^2 and 246 ± 7 kN/m^2, respectively, n = 6 per group). At 3 mo post-tamoxifen exposure, however, the forces generated by muscles of inducible DG KO mice (206 ± 8 kN/m^2, n = 5) were subtly but significantly ($P < 0.05$) lower than both those at the earlier time points and those for muscles of control mice at 3 mo (237 ± 10 kN/m^2, n = 5). Increased susceptibility to contraction-induced injury was observed at 2 mo and remained at 3 mo (Fig. 2 and Table S1). These results indicated that the increase in sensitivity to contraction-induced injury precedes necrosis, suggesting that this injury is a direct result of DGC disruption rather than a secondary consequence of necrosis or developmental defects.

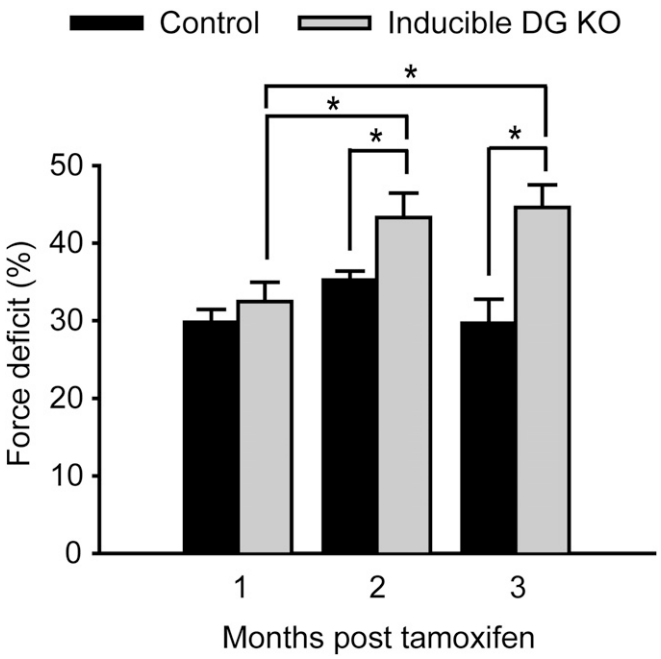

Fig. 2. Increased susceptibility to contraction-induced injury accompanies the reduction in DG levels. Shown are contraction-induced force deficits for EDL muscles (n = 5–9 per group) at various time points after exposure to tamoxifen. Values are means ± SE; *$P < 0.05$.

PHYSIOLOGY

Evidence of Titin Disruption Rather than Increased Sarcolemma Damage or Excitation–Contraction Uncoupling Followed the Lengthening Contractions. To evaluate whether sarcolemmal damage contributed to increased susceptibility to contraction-induced injury, several experiments were performed in inducible DG KO mice. In dystrophic muscles, damage mediated by extracellular calcium or reactive oxygen species is a consequence of increased membrane permeability (28–30). Exposure of muscles of *mdx* mice to either calcium-free buffer or buffer supplemented with the antioxidant *N*-acetylcysteine (NAC) decreased contraction-induced force deficits to 50% of those in control buffer (Fig. 3*A* and Table S2), confirming earlier reports regarding *mdx* mice (28–31). In contrast, muscles of inducible DG KO mice were unresponsive to the conditions of calcium-free buffer and antioxidant supplementation (Fig. 3*A* and Table S2). To test membrane permeability more directly, Evans Blue Dye (EBD) uptake was quantified for muscle, both at rest and after completing a lengthening contraction protocol (LCP) (Fig. 3*B*). Although a contraction-induced increase in EBD uptake was observed in muscles of *mdx* mice, no such increase was detected in muscles of inducible DG KO mice. These results indicated that the sarcolemma of the inducible DG KO mouse maintained its integrity during the LCP.

A demanding protocol of lengthening contractions induces excitation–contraction uncoupling in muscles of WT mice (32, 33). To test whether heightened excitation–contraction uncoupling accounted for increased contraction-induced force deficits in the muscles of inducible DG KO mice, post-LCP forces were measured in the presence and absence of 10 mM caffeine (Fig. 3*C* and Table S3); caffeine at this concentration increases sarcoplasmic release of Ca^{2+} during muscle activation (32, 33). The presence of caffeine decreased the force deficits in both the control and inducible DG KO mice, which is consistent with a deficit in calcium release from the sarcoplasmic reticulum. However, the two-factor ANOVA interaction term (i.e., genotype × caffeine status) was not significant ($P = 0.48$), and no significant differences were observed between control and inducible DG KO mice with respect to the extent to which caffeine diminished the force deficits (by 40 ± 6% for control mice, and by 35 ± 8% for inducible DG KO mice). These results suggested that excitation–contraction uncoupling does not account for the increased susceptibility to contraction-induced injury in the muscles of the inducible DG KO mice.

Passive elements of the sarcomeric cytoskeleton, such as titin, are susceptible to damage from lengthening contractions (31, 34).

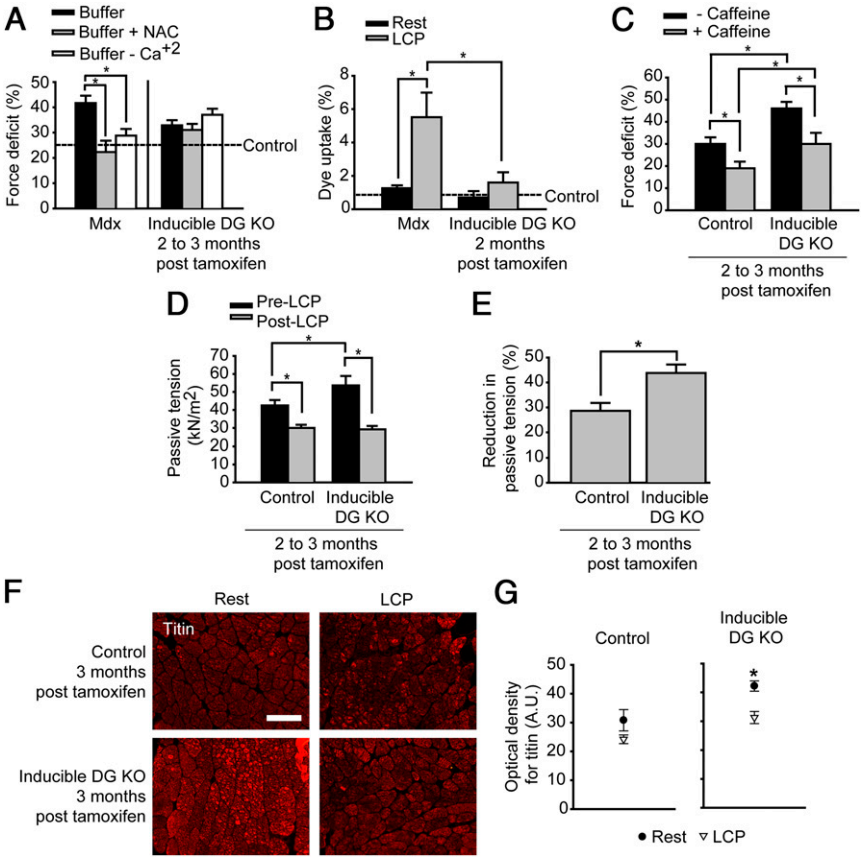

Fig. 3. Evidence for passive element disruption rather than excitation–contraction uncoupling or sarcolemma permeability as underlying the increased susceptibility to contraction-induced injury with DG knockdown. The EDL muscles of inducible DG KO mice were evaluated 2–3 mo after exposure to tamoxifen. (*A*) The antioxidant, *N*-acetylcysteine (NAC) or calcium-free buffer decreased the contraction-induced force deficits of *mdx* mice ($n = 5$–9 per group), but not those of the inducible DG KO mice ($n = 5$–6 per group). The mean control level (dashed line) was measured for control mice ($n = 5$) under normal buffer conditions. (*B*) Contraction-induced Evans Blue Dye uptake was increased in *mdx* mice ($n = 5$), but not in inducible DG KO mice ($n = 6$). The mean dye uptake for control muscle was quantified under rest conditions (dashed line). (*C*) The administration of caffeine led to comparable decreases in force deficits in muscles of control and inducible DG KO mice ($n = 5$ per group). (*D*) Passive tension occurred at 115% of optimal fiber length (L_o) before and after the lengthening contraction protocol (LCP) ($n = 8$ per group). (*E*) Passive tension was reduced at 115% of L_o, which was defined as the difference in passive tension pre- and post-LCP, and was expressed as the percentage of pre-LCP passive tension ($n = 8$ per group), $P = 0.003$. (*F*) Titin immunofluorescence in cryosections of muscles at rest and muscles after the LCP. (Scale bar: 100 μm.) (*G*) For muscles 2–3 mo post-tamoxifen exposure, optical density measures of titin immunofluorescence in cryosections were quantified for control and inducible DG KO mice ($n = 3$ per group). Comparison of muscles exposed to the LCP with those at rest revealed a significant difference exclusively for inducible DG KO mice, $P = 0.0009$. Values are means ± SE; $^*P < 0.05$.

To investigate this phenomenon in our model, passive tension at 115% of optimal muscle fiber length was determined pre- and post-LCP (Fig. 3*D* and Table S4). Before the LCP, passive tensions for inducible DG KO muscles were 1.3-fold greater than for control muscles ($P = 0.029$). The LCP induced a reduction in passive tension, which was more severe for the muscles of inducible DG KO mice than for those of control mice, as confirmed by a significant ($P = 0.02$) two-factor ANOVA interaction term between genotype and LCP exposure (Fig. 3*E*). Titin expression was investigated by observing immunofluorescence in transverse muscle sections (Fig. 3*F*). In the case of muscles at rest, titin immunofluorescence in the inducible DG KO muscles was high, which was consistent with high pre-LCP passive tension observed in inducible DG KO muscles. For muscles subjected to the LCP, the optical density of titin (by 26%) decreased relative to that in muscles at rest exclusively in the muscles of inducible DG KO mice, $P = 0.0009$ (Fig. 3*G*). These findings indicate that a decrease in DG levels is accompanied by a compensatory increase in titin levels at rest, but that, in the context of lengthening contractions, this increase is insufficient to prevent a loss of titin and the development of severe force deficits. We also investigated the immunofluorescence levels of desmin, nebulin, and α-actinin in muscle sections. In contrast with the data regarding titin, optical density values for desmin, nebulin, and α-actinin were unaltered by the LCP, thereby implying that the extent of disruption among cytoskeletal/sarcomeric components is variable (Table S5).

Increased Susceptibility to Contraction-Induced Injury Is Prevented by Maintaining WT Levels of β-DG and Core α-DG Expression. To determine which domain of DG accounts for increased susceptibility to injury, we investigated an additional mouse model—the inducible α-DG$^{\Delta N\text{-term}}$ mouse. This model enabled us to examine the effects of selectively maintaining levels of β-DG and core α-DG while reducing those of the glycosylated form of α-DG that is required for binding to the extracellular matrix (i.e., functionally glycosylated α-DG). In these animals, tamoxifen exposure leads to the replacement of a subpopulation of fully glycosylated α-DG with α-DG lacking the N-terminal domain, which is essential for glycosylation by the LARGE enzyme. No muscle pathology was observed in these mice after tamoxifen exposure. Levels of glycosylated α-DG, as assessed using the IIH6 glyco-specific antibody, were reduced to levels comparable with those in muscles of inducible α-DG$^{\Delta N\text{-term}}$ mice and inducible DG KO mice (Fig. S4*A*). By 2 mo post-tamoxifen exposure, levels of β-DG, core α-DG, and dystrophin differed between the two models—the levels were reduced in muscles of tamoxifen-exposed inducible DG KO mice, but not in muscles of inducible α-DG$^{\Delta N\text{-term}}$ mice (Fig. 1 and Fig. S4*A*). At 2–3 mo post-tamoxifen, no differences in specific force were observed in the muscles of inducible α-DG$^{\Delta N\text{-term}}$ mice (247 ± 15 kN/m^2, $n = 5$) vs. control mice (268 ± 15 kN/m^2, $n = 5$). In contrast with the inducible DG KO mice, which exhibited a high level of contraction-induced force deficits, the α-DG$^{\Delta N\text{-term}}$ mice generated forces comparable with those observed in controls (Fig. S4*B* and Table S6). These results indicate that preservation of the expression of core α-DG, β-DG, and dystrophin is sufficient to prevent severe contraction-induced force deficits.

Discussion

The association of heightened contraction-induced injury with DGC-related muscular dystrophies was established more than 20 y ago (22, 25, 26). Based on these early reports, the DGC was proposed to directly limit susceptibility to contraction-induced injury, and this injury was proposed as a primary trigger of disease onset. However, more recent reports have raised the possibility that the extent of contraction-induced injury may be affected indirectly by the absence of the DGC. Specifically, they demonstrated that, during either development or cycles of degeneration/regeneration, lack of the DGC leads to deleterious outcomes, such as inflammatory signaling (35, 36) or abnormal localization/function of caveolae (37), membrane-bound enzyme complexes (38, 39), and ion channels (40–42). These features have the potential to alter calcium influx/handling, the levels of reactive oxygen species, and cellular signaling, thereby exacerbating contraction-induced injury by increasing permeability of the sarcolemma, intensifying reactive oxygen species/calcium-mediated damage, and reducing release of calcium from the sarcoplasmic reticulum calcium (43). In the present study, we have demonstrated that, when a reduction in DG levels is induced at maturity, increased susceptibility to contraction-induced injury occurs in the absence of overt necrosis, which is consistent with a direct role for the DGC in limiting contraction-induced injury independent of development or necrosis.

We have also demonstrated that the stability of titin, rather than sarcolemmal integrity or excitation contraction coupling, is especially sensitive to reductions in levels of DG and the DGC at maturity. Lastly, this work demonstrates that preservation of the levels of β-DG in the context of reduced levels of the fully glycosylated form of α-DG prevents both disruption of the DGC and increased contraction-induced injury, which implies that α- and β-DG have distinct roles and are required at different levels—with α-DG preserving sarcolemmal integrity and being required in only minimal amounts, and β-DG stabilizing dystrophin and the sarcomeric cytoskeleton and being required in greater amounts. These findings suggest that the cytoskeleton of mature muscle is especially sensitive to reductions in DG levels.

The roles of DG and the DGC in contraction-induced injury were previously investigated in mouse models in which a genetic defect was present throughout development. During this process and the accompanying growth, skeletal muscle fibers increase significantly in breadth (the mean diameter of hind limb muscle fibers increases fivefold) and even more in length (the average muscle fiber length for an adult is 20–30 mm, which is 1,000-fold longer than a mononucleated cell) (44). DG and the DGC are critical during this dynamic phase of sarcolemmal expansion (45–47). Contraction-induced injury before the onset of necrosis has been investigated in muscles of mouse pups deficient for both dystrophin and utrophin (48). β-DG is able to bind each of these proteins, and a deficiency for both completely eliminates the link between β-DG and the cytoskeleton. Muscles from mouse pups with such a deficiency sustained twofold greater force deficits than muscles from control mice in the absence of necrosis (48). These results complement the present research. In the present investigation, the separation of susceptibility to contraction-induced injury and necrosis was established at reduced DGC levels rather than abolished levels. Because comparable results were observed in the previous research regarding mouse pups completely deficient in intact DGC levels, the indication is that the onset of increased injury precedes muscle degeneration when intact DGC levels are compromised in general (i.e., significantly reduced or completely absent) (48). The present study furthers the previous findings by investigating the susceptibility to contraction-induced injury at maturity. Because the dystrophin-deficient pups developed in the absence of an intact DGC, it could not be determined in that study whether the increased contraction-induced injury was a consequence of abnormal development rather than a more direct result of DGC disruption. In the present study, induction of the knockdown in mature mice demonstrates that the DGC can restrict injury independently of the effects of the DGC on development.

Various inducible systems have been used to study the histopathology that results from disrupting the DGC. These systems include tamoxifen-induced disruption of fukutin (46), RNA-mediated knockdown of fukutin-related protein (49), and dystrophin knockdown using a tetracycline-responsive transactivator or RNAi system (50, 51). Interestingly, knockdown of dystrophin at maturity did not result in a discernible phenotype (48). However, these investigations were limited, in that only histology, and not muscle function, was tested. In the present study, we found that a reduction in

sarcolemmal expression of dystrophin accompanied DG knockdown. Such a reduction is expected to have had a major impact on the results for contraction-induced injury in the present study because dystrophin links DG to the cytoskeleton, and dystrophin deficiency in other mouse models exacerbates contraction-induced force deficits (22, 25–27). Therefore, the data of the present study suggest that increased contraction-induced injury susceptibility was present in the past studies regarding dystrophin knockdown at maturity but were simply not detected because analysis was restricted to histological assessment alone. This possibility demonstrates the importance of complementing histological analysis with physiology measures when performing research on skeletal muscle.

Results of the present study support the concept that, in the context of an intact DGC, only minimal levels of glycosylated α-DG are required for limiting contraction-induced injury. When we reduced levels of the fully glycosylated form of α-DG using the inducible α-DG$^{\Delta N\text{-term}}$ mouse model, susceptibility to contraction-induced injury remained at WT levels. This finding is consistent with a previous report showing that low amounts of intact α-DG are necessary for preserving the function of receptors on the basal lamina—a feature that is essential for maintaining the integrity of the sarcolemma (52). For example, muscles of knock-in mice carrying a retrotransposon insertion of the gene encoding fukutin maintained only a small level of α-DG hypoglycosylation yet retained 50% of their laminin-binding capacity, whereas mice null for the glycosyltransferase LARGE (*Large^{myd}* mice), in which glycosylated α-DG was absent, retained less than 5% of laminin-binding capacity (52). Also, the extracellular matrix receptor α7β1 integrin is thought to help preserve the integrity of the basal lamina and limit contraction-induced injury, especially when α-DG function is disrupted (24).

Notwithstanding the lack of evidence for sarcolemma fragility in the muscles of inducible DG KO mice, instability of myofibrillar cytoskeleton was evident from the contraction-induced decrease in titin immunostaining and the reduction in passive tension. In a relevant report, muscles of *mdx* and WT mice were exposed to lengthening contractions in vivo, and then individual, permeabilized fibers from these muscles were tested (27). These muscle fibers were activated by direct addition of calcium to the buffer, thereby bypassing the sarcolemma and excitation–contraction coupling. The finding that, for *mdx* mice, permeabilized fibers from injured muscles generated 28% less force than fibers from uninjured muscles indicated that myofibrillar disruption contributed to the contraction-induced injury. Myofibrillar disruption would help explain why contraction-induced force deficits typically exceed the extent predicted based on the uptake of procion orange dye or EBD, indicators of breaches of the sarcolemma, in *mdx* muscle (22, 28, 40, 53). The extent of disruption of distinct components of the cytoskeleton/sarcomere may be unequal, as suggested by our finding that the expression of titin was disrupted by lengthening contractions whereas that of desmin, nebulin, and α-actinin was unperturbed. Our data are consistent with two other reports describing abnormal titin staining and reduced passive tension in WT muscle after lengthening contractions (31, 34), as well as with the fact that titin fragmentation is detected in serum and urine, in dystrophin-deficient mice as well as Duchenne muscular dystrophy patients (54–56). Disruption of the DGC is accompanied by compromised lateral force transmission (31, 34). Thus, the excessive reduction in titin staining in muscles of the inducible DG KO mice may have been due to excessive strain on titin during contractions, when such transmission was disrupted. Therefore, our results are consistent with a mechanism of contraction-induced injury whereby the ability to laterally shunt tension to β-DG is decreased, resulting in the development of excessive tension in specific components of the sarcomeric cytoskeleton.

The finding that the DGC limits contraction-induced injury in mature muscle has implications for approaches to the treatment of muscular dystrophy. One is that it would likely be beneficial to extend therapeutic treatment into maturity. Previous reports describing a delay in the onset of histopathology (up to 1 y) after disruption of the DGC in mature mice led to the proposal that infrequent treatment may be sufficient at maturity (15). In the present work, the finding that increased susceptibility to contraction-induced injury occurs in the absence of necrosis when the DGC is compromised at maturity stresses the necessity to treat the disease frequently. In addition, the finding that the sarcomeric cytoskeleton protein titin is especially sensitive to contraction-induced damage when DGC levels are reduced provides a better understanding of the pathophysiology, which will facilitate the development of more effective therapeutic strategies.

Materials and Methods

Refer to *SI Materials and Methods* for details regarding mice, antibodies, reagents, and analysis.

Inducible Mouse Models. All mice were maintained at The University of Iowa Animal Care Unit, and the animal studies were authorized by the Animal Care Use and Review Committee of The University of Iowa. Mice homozygous for a floxed allele of DG, in which loxP sites flank exon 4 of *Dag1* (49–51), were crossed with transgenic mice with a tamoxifen-inducible cre-mediated recombination system (004682; The Jackson Laboratory). This recombination system was driven by the chicken β-actin promoter/enhancer coupled with the cytomegalovirus (CMV) immediate-early enhancer. Male offspring heterozygous for the floxed allele and Cre-positive were crossed with female mice heterozygous for the floxed allele. Inducible DG KO mice were obtained from this cross. Control mice were Cre-negative and homozygous for floxed *Dag1*. Inducible α-DG$^{\Delta N\text{-term}}$ mice were obtained by crossing cre-positive male mice heterozygous for floxed *Dag1* with mice heterogeneous for deletion of the N-terminal domain of α-DG. At 10–12 wk of age, mice were gavaged with tamoxifen (200 mg/kg) on two occasions within a 1-wk period.

Measurement of Contractile Properties. At various time points after *Dag1* disruption, contractile properties of extensor digitorum longus (EDL) muscles were assessed ex vivo (45). Mice were anesthetized before surgical removal of the EDL. Muscle mass, fiber length, and maximum isometric tetanic force were measured. These measurements were used to determine total cross-sectional area and specific force (kN/m^2) (53, 57). The susceptibility to contraction-induced injury was determined after lengthening contractions. Differences between control and inducible DG KO mice were assessed by analysis of variance testing. Muscles were prepared for immunofluorescence or Western blot analysis as described in *SI Materials and Methods*.

ACKNOWLEDGMENTS. We thank the K.P.C. laboratory and C. Blaumueller for discussions. This work was supported by Paul D. Wellstone Muscular Dystrophy Cooperative Research Center Grant 1U54NS053672 (to K.P.C.); Muscular Dystrophy Association Grant MDA3936 (to K.P.C.); a Muscular Dystrophy Association Development grant (to E.P.R.); National Center of Neurology and Psychiatry Intramural Research Grant 26-8 for Neurological and Psychiatric Disorders (to F.S.); Grants-in-Aid for Scientific Research from the Ministry of Education, Culture, Sports, Science and Technology (C)26461281 (to F.S.) and (C)16K09682 (to K.M.); Iowa Cardiovascular Center Institutional Research Fellowship Grant NIH 5T32HL007121-37 (to R.T.); and US Department of Defense Grant W81XWH-05-1-0079 (to K.P.C.). K.P.C. is an Investigator of the Howard Hughes Medical Institute.

1. Durbeej M, Campbell KP (2002) Muscular dystrophies involving the dystrophin-glycoprotein complex: An overview of current mouse models. *Curr Opin Genet Dev* 12(3):349–361.
2. Davies KE, Nowak KJ (2006) Molecular mechanisms of muscular dystrophies: Old and new players. *Nat Rev Mol Cell Biol* 7(10):762–773.
3. Duclos F, et al. (1998) Progressive muscular dystrophy in alpha-sarcoglycan-deficient mice. *J Cell Biol* 142(6):1461–1471.
4. Durbeej M, et al. (2000) Disruption of the beta-sarcoglycan gene reveals pathogenetic complexity of limb-girdle muscular dystrophy type 2E. *Mol Cell* 5(1):141–151.
5. Straub V, et al. (1998) Molecular pathogenesis of muscle degeneration in the delta-sarcoglycan-deficient hamster. *Am J Pathol* 153(5):1623–1630.
6. Ervasti JM, Ohlendieck K, Kahl SD, Gaver MG, Campbell KP (1990) Deficiency of a glycoprotein component of the dystrophin complex in dystrophic muscle. *Nature* 345(6273):315–319.

7. Ohlendieck K, Campbell KP (1991) Dystrophin-associated proteins are greatly reduced in skeletal muscle from mdx mice. *J Cell Biol* 115(6):1685–1694.
8. Matsumura K, et al. (1993) Mild deficiency of dystrophin-associated proteins in Becker muscular dystrophy patients having in-frame deletions in the rod domain of dystrophin. *Am J Hum Genet* 53(2):409–416.
9. Di Blasi C, et al. (1996) Dystrophin-associated protein abnormalities in dystrophin-deficient muscle fibers from symptomatic and asymptomatic Duchenne/Becker muscular dystrophy carriers. *Acta Neuropathol* 92(4):369–377.
10. Hara Y, et al. (2011) A dystroglycan mutation associated with limb-girdle muscular dystrophy. *N Engl J Med* 364(10):939–946.
11. Ibraghimov-Beskrovnaya O, et al. (1992) Primary structure of dystrophin-associated glycoproteins linking dystrophin to the extracellular matrix. *Nature* 355(6362):696–702.
12. Barresi R, Campbell KP (2006) Dystroglycan: From biosynthesis to pathogenesis of human disease. *J Cell Sci* 119(Pt 2):199–207.
13. Yoshida-Moriguchi T, et al. (2010) O-mannosyl phosphorylation of alpha-dystroglycan is required for laminin binding. *Science* 327(5961):88–92.
14. Rybakova IN, Patel JR, Ervasti JM (2000) The dystrophin complex forms a mechanically strong link between the sarcolemma and costameric actin. *J Cell Biol* 150(5):1209–1214.
15. Ramaswamy KS, et al. (2011) Lateral transmission of force is impaired in skeletal muscles of dystrophic mice and very old rats. *J Physiol* 589(Pt 5):1195–1208.
16. Dinçer P, et al. (2003) A novel form of recessive limb girdle muscular dystrophy with mental retardation and abnormal expression of alpha-dystroglycan. *Neuromuscul Disord* 13(10):771–778.
17. Geis T, et al. (2013) Homozygous dystroglycan mutation associated with a novel muscle-eye-brain disease-like phenotype with multicystic leucodystrophy. *Neurogenetics* 14(3-4):205–213.
18. Willer T, et al. (2012) ISPD loss-of-function mutations disrupt dystroglycan O-mannosylation and cause Walker-Warburg syndrome. *Nat Genet* 44(5):575–580.
19. Yoshida-Moriguchi T, Campbell KP (2015) Matriglycan: A novel polysaccharide that links dystroglycan to the basement membrane. *Glycobiology* 25(7):702–713.
20. Godfrey C, Foley AR, Clement E, Muntoni F (2011) Dystroglycanopathies: Coming into focus. *Curr Opin Genet Dev* 21(3):278–285.
21. Han R, et al. (2009) Basal lamina strengthens cell membrane integrity via the laminin G domain-binding motif of alpha-dystroglycan. *Proc Natl Acad Sci USA* 106(31): 12573–12579.
22. Petrof BJ, Shrager JB, Stedman HH, Kelly AM, Sweeney HL (1993) Dystrophin protects the sarcolemma from stresses developed during muscle contraction. *Proc Natl Acad Sci USA* 90(8):3710–3714.
23. Claflin DR, Brooks SV (2008) Direct observation of failing fibers in muscles of dystrophic mice provides mechanistic insight into muscular dystrophy. *Am J Physiol Cell Physiol* 294(2):C651–C658.
24. Gumerson JD, Kabaeva ZT, Davis CS, Faulkner JA, Michele DE (2010) Soleus muscle in glycosylation-deficient muscular dystrophy is protected from contraction-induced injury. *Am J Physiol Cell Physiol* 299(6):C1430–C1440.
25. Weller B, Karpati G, Carpenter S (1990) Dystrophin-deficient mdx muscle fibers are preferentially vulnerable to necrosis induced by experimental lengthening contractions. *J Neurol Sci* 100(1-2):9–13.
26. Moens P, Baatsen PH, Maréchal G (1993) Increased susceptibility of EDL muscles from mdx mice to damage induced by contractions with stretch. *J Muscle Res Cell Motil* 14(4):446–451.
27. Blaauw B, et al. (2010) Eccentric contractions lead to myofibrillar dysfunction in muscular dystrophy. *J Appl Physiol (1985)* 108(1):105–111.
28. Whitehead NP, Pham C, Gervasio OL, Allen DG (2008) N-Acetylcysteine ameliorates skeletal muscle pathophysiology in mdx mice. *J Physiol* 586(7):2003–2014.
29. Yeung EW, et al. (2005) Effects of stretch-activated channel blockers on [Ca2+]i and muscle damage in the mdx mouse. *J Physiol* 562(Pt 2):367–380.
30. Ng R, Metzger JM, Claflin DR, Faulkner JA (2008) Poloxamer 188 reduces the contraction-induced force decline in lumbrical muscles from mdx mice. *Am J Physiol Cell Physiol* 295(1):C146–C150.
31. Zhang BT, Yeung SS, Allen DG, Qin L, Yeung EW (2008) Role of the calcium-calpain pathway in cytoskeletal damage after eccentric contractions. *J Appl Physiol (1985)* 105(1):352–357.
32. Ingalls CP, Warren GL, Zhang JZ, Hamilton SL, Armstrong RB (2004) Dihydropyridine and ryanodine receptor binding after eccentric contractions in mouse skeletal muscle. *J Appl Physiol (1985)* 96(5):1619–1625.
33. Warren GL, et al. (1993) Excitation failure in eccentric contraction-induced injury of mouse soleus muscle. *J Physiol* 468:487–499.
34. Zhang BT, et al. (2012) Pathways of Ca^{2+} entry and cytoskeletal damage following eccentric contractions in mouse skeletal muscle. *J Appl Physiol (1985)* 112(12): 2077–2086.
35. Chen YW, et al. (2005) Early onset of inflammation and later involvement of TGFbeta in Duchenne muscular dystrophy. *Neurology* 65(6):826–834.
36. Pescatori M, et al. (2007) Gene expression profiling in the early phases of DMD: A constant molecular signature characterizes DMD muscle from early postnatal life throughout disease progression. *FASEB J* 21(4):1210–1226.
37. Shibuya S, Wakayama Y, Inoue M, Oniki H, Kominami E (2002) Changes in the distribution and density of caveolin 3 molecules at the plasma membrane of mdx mouse skeletal muscles: A fracture-label electron microscopic study. *Neurosci Lett* 325(3):171–174.
38. Whitehead NP, Yeung EW, Froehner SC, Allen DG (2010) Skeletal muscle NADPH oxidase is increased and triggers stretch-induced damage in the mdx mouse. *PLoS One* 5(12):e15354.
39. Ismail HM, Scapozza L, Ruegg UT, Dorchies OM (2014) Diapocynin, a dimer of the NADPH oxidase inhibitor apocynin, reduces ROS production and prevents force loss in eccentrically contracting dystrophic muscle. *PLoS One* 9(10):e110708.
40. Whitehead NP, Streamer M, Lusambili LI, Sachs F, Allen DG (2006) Streptomycin reduces stretch-induced membrane permeability in muscles from mdx mice. *Neuromuscul Disord* 16(12):845–854.
41. Gervásio OL, Whitehead NP, Yeung EW, Phillips WD, Allen DG (2008) TRPC1 binds to caveolin-3 and is regulated by Src kinase: Role in Duchenne muscular dystrophy. *J Cell Sci* 121(Pt 13):2246–2255.
42. Hirn C, Shapovalov G, Petermann O, Roulet E, Ruegg UT (2008) Nav1.4 deregulation in dystrophic skeletal muscle leads to Na+ overload and enhanced cell death. *J Gen Physiol* 132(2):199–208.
43. Allen DG, Whitehead NP, Froehner SC (2016) Absence of dystrophin disrupts skeletal muscle signaling: Roles of Ca2+, reactive oxygen species, and nitric oxide in the development of muscular dystrophy. *Physiol Rev* 96(1):253–305.
44. Grounds MD, Shavlakadze T (2011) Growing muscle has different sarcolemmal properties from adult muscle: a proposal with scientific and clinical implications: Reasons to reassess skeletal muscle molecular dynamics, cellular responses and suitability of experimental models of muscle disorders. *BioEssays* 33(6):458–468.
45. Cohn RD, et al. (2002) Disruption of DAG1 in differentiated skeletal muscle reveals a role for dystroglycan in muscle regeneration. *Cell* 110(5):639–648.
46. Beedle AM, et al. (2012) Mouse fukutin deletion impairs dystroglycan processing and recapitulates muscular dystrophy. *J Clin Invest* 122(9):3330–3342.
47. Janke A, Upadhaya R, Snow WM, Anderson JE (2013) A new look at cytoskeletal NOS-1 and β-dystroglycan changes in developing muscle and brain in control and mdx dystrophic mice. *Dev Dyn* 242(12):1369–1381.
48. Grange RW, Gainer TG, Marschner KM, Talmadge RJ, Stull JT (2002) Fast-twitch skeletal muscles of dystrophic mouse pups are resistant to injury from acute mechanical stress. *Am J Physiol Cell Physiol* 283(4):C1090–C1101.
49. Wang CH, et al. (2011) Post-natal knockdown of fukutin-related protein expression in muscle by long-termRNA interference induces dystrophic pathology [corrected]. *Am J Pathol* 178(1):261–272, and erratum (2011) 178(3):1406.
50. Ghahramani Seno MM, et al. (2008) RNAi-mediated knockdown of dystrophin expression in adult mice does not lead to overt muscular dystrophy pathology. *Hum Mol Genet* 17(17):2622–2632.
51. Ahmad A, Brinson M, Hodges BL, Chamberlain JS, Amalfitano A (2000) Mdx mice inducibly expressing dystrophin provide insights into the potential of gene therapy for duchenne muscular dystrophy. *Hum Mol Genet* 9(17):2507–2515.
52. Kanagawa M, et al. (2009) Residual laminin-binding activity and enhanced dystroglycan glycosylation by LARGE in novel model mice to dystroglycanopathy. *Hum Mol Genet* 18(4):621–631.
53. Consolino CM, Brooks SV (2004) Susceptibility to sarcomere injury induced by single stretches of maximally activated muscles of mdx mice. *J Appl Physiol (1985)* 96(2):633–638.
54. Hathout Y, et al. (2014) Discovery of serum protein biomarkers in the mdx mouse model and cross-species comparison to Duchenne muscular dystrophy patients. *Hum Mol Genet* 23(24):6458–6469.
55. Hathout Y, et al. (2016) Clinical utility of serum biomarkers in Duchenne muscular dystrophy. *Clin Proteomics* 13:9.
56. Rouillon J, et al. (2014) Proteomics profiling of urine reveals specific titin fragments as biomarkers of Duchenne muscular dystrophy. *Neuromuscul Disord* 24(7):563–573.
57. Mendias CL, Marcin JE, Calerdon DR, Faulkner JA (2006) Contractile properties of EDL and soleus muscles of myostatin-deficient mice. *J Appl Physiol (1985)* 101(3):898–905.
58. Han R, Rader EP, Levy JR, Bansal D, Campbell KP (2011) Dystrophin deficiency exacerbates skeletal muscle pathology in dysferlin-null mice. *Skelet Muscle* 1(1):35.
59. Cairns SP, Chin ER, Renaud JM (2007) Stimulation pulse characteristics and electrode configuration determine site of excitation in isolated mammalian skeletal muscle: implications for fatigue. *J Appl Physiol (1985)* 103(1):359–368.
60. Kobayashi YM, et al. (2008) Sarcolemma-localized nNOS is required to maintain activity after mild exercise. *Nature* 456(7221):511–515.
61. Anderson LV, Davison K (1999) Multiplex Western blotting system for the analysis of muscular dystrophy proteins. *Am J Pathol* 154(4):1017–1022.

Supporting Information

Rader et al. 10.1073/pnas.1605265113

SI Materials and Methods

Inducible Mouse Models. All mice were maintained at The University of Iowa Animal Care Unit, and the animal studies were authorized by the Animal Care Use and Review Committee of The University of Iowa. Mice homozygous for a floxed allele of dystroglycan (DG), in which loxP sites flank exon 4 of *Dag1* (49, 50), were crossed with transgenic mice with a tamoxifen-inducible cre-mediated recombination system (004682; The Jackson Laboratory). This recombination system was driven by the chicken β-actin promoter/enhancer coupled with the cytomegalovirus (CMV) immediate-early enhancer. Male offspring heterozygous for the floxed allele and Cre-positive were crossed with female mice heterozygous for the floxed allele. Inducible DG KO mice were obtained from this cross. Control mice were Cre-negative and homozygous for floxed *Dag1*.

For the generation of inducible α-DG$^{\Delta N\text{-term}}$ mice, *Dag1* exon 3, which contains the ATG initiation codon, was replaced with a construct containing the *Dag1* Δ31 ∼314-aa cDNA, SV40polyA, and the loxP-Neo cassette. The linearized targeting vector was electroporated into C57BL/6 embryonic stem cells. G418-resistant ES-targeted clones were isolated and confirmed by PCR and Southern blotting analysis on both arms of homology with gene-specific probes. In addition, a Neo probe was used to screen for random insertion events. Chimeras were generated by injecting the positive ES cells into blastocysts of BALB/c mice and identified by coat color. Chimeras were mated to C57BL/6J females to generate F1 heterozygous mice. Inducible α-DG$^{\Delta N\text{-term}}$ mice were obtained by crossing cre-positive male mice heterozygous for floxed *Dag1* with mice heterogeneous for deletion of the N-terminal domain of α-DG. At 10–12 wk of age, inducible α-DG$^{\Delta N\text{-term}}$ mice and inducible DG KO mice were gavaged with tamoxifen (200 mg/kg) on two occasions within a 1-wk period.

Measurement of Contractile Properties. To compare the contractile properties of muscles of the inducible DG KO mice at various times post-tamoxifen induction, EDL muscles were surgically removed and analyzed (53, 57). The muscle was submerged in an oxygenated (95% oxygen, 5% carbon dioxide) buffer solution (pH 7.4) maintained at 25 °C: 137 mM NaCl, 5 mM KCl, 2 mM $CaCl_2$, 1 mM $MgSO_4$, 1 mM NaH_2PO_4, 24 mM $NaHCO_3$, 11 mM glucose, and 0.025 mM tubocurarine chloride. The proximal tendon was clamped to a post, and the distal tendon was tied to a dual mode servomotor (Model 305C; Aurora Scientific). Optimal current and muscle length (L_o) were determined by monitoring isometric twitch force. Fiber length (L_f) was determined using the L_o-to-L_f ratio of 0.45 (53, 57). Optimal frequency and maximal isometric tetanic force were determined. The muscle was then subjected to a lengthening contraction protocol (LCP) consisting of eight lengthening contractions separated by 3-min intervals. In previous research, this protocol was effective at revealing differences in LCP-induced force deficits among closely related dystrophic mouse models (58). Each lengthening contraction consisted of an initial 100-ms isometric contraction at optimal frequency, immediately followed by a stretch from L_o to 30% of L_f beyond L_o at a velocity of 1 L_f/s at optimal frequency. The muscle was then passively returned to L_o at the same velocity. At 30–45 min after the LCP, isometric tetanic force was measured, and force deficit was calculated as the decrease in isometric tetanic force post-LCP as a percentage of pre-LCP isometric tetanic force. The force deficit was stable during this time period (e.g., force deficits were 44 ± 3% at both 30 min and 45 min after the LCP for inducible DG KO mice 2 mo post-tamoxifen, n = 8–9) and reflected a persistent phenomenon rather than a transient feature like those that have been observed in multiple muscular dystrophy models at early time points post-LCP (58). After the contractile properties were analyzed, muscle mass was measured. Muscle mass, L_f, and pre-LCP isometric force were used to determine specific force (kN/m^2) (53, 57).

To assess the effectiveness of antioxidants, calcium-free conditions, or caffeine potentiation in the muscles of inducible DG KO mice and to compare the susceptibility to contraction-induced injury of muscles of inducible α-DG$^{\Delta N\text{-term}}$ mice with that of inducible DG KO mice and control mice, muscles were subjected to a modified version of a previously described LCP (28). This protocol was previously shown to be sensitive to differences in injury susceptibility due to membrane fragility/permeability, to the production of reactive oxygen species, and to treatment with antioxidants in *mdx* mice (28). The EDL muscle was isolated and submerged in Tyrode solution (at room temperature, 22 °C) (28). The optimal current, L_o, and maximal isometric tetanic force were determined (120 Hz). For the antioxidant and calcium-free experiments of inducible DG KO mice and the testing for inducible α-DG$^{\Delta N\text{-term}}$ mice relative to inducible DG KO mice, the solution was then replaced with a modified Tyrode buffer-Tyrode solution plus 0.02% (wt/vol) Evans Blue dye (EBD) and 0.5% bovine serum albumin with or without 20 mM NAC. After 30 min, force was measured again to confirm stable conditions. For the calcium-free experiment, the buffer was then replaced with Tyrode solution without calcium (the concentration of magnesium was increased to 2.3 mM to maintain divalent cation concentration), 0.02% (wt/vol) EBD, and 0.5% bovine serum albumin. The temperature was set to 35 °C for the remainder of the experiment. The muscle was then subjected to an LCP consisting of three lengthening contractions at 30-s intervals. The tetani of each contraction had a duration of 300 ms and a frequency of 120 Hz. Beginning 150 ms after the start of the tetani, the muscle was stretched from L_o to 30% L_f beyond L_o at a velocity of 1 L_f/s, and then immediately returned to L_o at the same velocity. For the calcium-free experiment, the solution was replaced with Tyrode solution (i.e., with calcium) 30 min after the LCP. At 1 h after the LCP, isometric tetanic force (120 Hz) was measured, and the force deficit was calculated as the decrease in isometric tetanic force post-LCP as a percentage of pre-LCP isometric tetanic force. For determination of caffeine potentiation, the investigator was blinded to mouse genotype. At 1 h post-LCP, the muscle was submerged in Tyrode solution with 10 mM caffeine. Muscles tested in vitro are activated via excitation–contraction coupling (59) and rely on sarcoplasmic release of Ca^{2+} during muscle activation. Ca^{2+} release increased with the concentration of caffeine tested (32, 33) and did not affect passive tension. After 5 min, the isometric tetanic force (120 Hz) was measured again to determine the force deficit in the presence of caffeine.

Passive tension was measured before and after muscle was subjected to a modified version of a previously described LCP (34), with the investigator blinded to mouse genotype. This protocol is effective at distinguishing changes in passive tension upon modulation of calcium entry (34). The right and left EDL muscles were isolated and submerged in oxygenated (95% oxygen, 5% carbon dioxide) buffer solutions (pH 7.4) maintained at room temperature: 137 mM NaCl, 5 mM KCl, 2 mM $CaCl_2$, 1 mM $MgSO_4$, 1 mM NaH_2PO_4, 24 mM $NaHCO_3$, 11 mM glucose, and 0.025 mM tubocurarine chloride. For control purposes, the left EDL was secured at a taut length throughout the experiment,

using insect pins and a plate coated with sylgard. The right EDL was tied to a dual-mode servomotor (Model 305C; Aurora Scientific) and subjected to the experimental protocol. L_o was determined while monitoring isometric twitch forces. The length of the muscle was then set to 90% of L_o, incrementally increased (by steps of 5% at a velocity 1 L_o/s and held for 1 min at each step) to 115% of L_o, and then returned to L_o. Passive tension was measured at the end of each 1-min interval before the next lengthening step. The muscle was then subjected to an LCP consisting of 10 lengthening contractions at 10-s intervals. For each lengthening contraction, the muscle was first activated (150 Hz) at a fixed length for 250 ms, lengthened to L_o plus 120% of L_o at a velocity of 1.3 L_o/s, and then passively returned to L_o. The isometric tetanic force was measured 1 min and 30 min after the LCP, and force deficit was calculated as the drop in force as a percentage of the force for the isometric phase of the first lengthening contraction. After 10 min, the resting passive tension was measured as was done before the LCP. The reduction in resting passive tension at 115% L_o was calculated as the difference in passive tension pre- and post-LCP and expressed as a percentage of the pre-LCP passive tension.

cDNA Synthesis and Real-Time PCR Assay. Total RNA was extracted from cells in culture using the RNeasy isolation kit (Qiagen). First-strand cDNA was synthesized from total RNA using AMV reverse transcriptase (Roche) and a 1:1 mix oligo $d(T)_{16}$:random hexamers, according to the manufacturer's instructions. The *Dag1* and *GAPDH* genes were real-time amplified from cDNA using oligonucleotides specific to each gene (*Dag1*-forward, 5′ TGGTTGGCATTCCAGACG; *Dag1*-reverse, 5′ TATGACTGTGTGGGTCCCAG; GAPDH-forward, 5′ AACAGGGTGGTGGACCTCAT; GAPDH-reverse, 5′ TTGGGATAGGGCCTCTCTTG). GAPDH was used as the normalization control. cDNA levels were determined using SYBR green in an MyiQ rt-PCR detection system (Bio-Rad). All samples were run in triplicate.

Histology and Immunofluorescence Analysis. Muscles were dissected, covered in embedding medium, flash frozen in isopentane (−160 °C), and stored at −80 °C. Cryosections (7 μm) from each muscle were used for hematoxylin/eosin staining or immunofluorescence (4). Sections were blocked with 3% BSA in PBS for 30 min and incubated with primary antibody overnight (4 °C). Antibodies against the core proteins of α- and β-DG and the laminin-binding glyco-epitope of DG were used (21, 60). The sections were then incubated for 30 min with Cy3-conjugated secondary antibodies (Molecular Probes). The percentage of centrally nucleated fibers and variability in muscle fiber area were determined for cryosections costained with anti-caveolin 3 antibody and 4′,6-diamidino-2-phenylindole (DAPI) (Sigma-Aldrich), using Image Pro Plus 6 and assessing the maximum number of nonoverlapping images obtained at 20× magnification. Variability in muscle fiber area was assessed by determining the coefficient of variance for each muscle section, as SD of muscle fiber area multiplied by 1,000 and divided by the mean muscle fiber area. For each muscle section, the immunofluorescence intensity for antibodies against the cytoskeletal/sarcomeric proteins titin (9D10; Developmental Studies Hybridoma Bank), desmin (D8281; Sigma), α-actinin (A7811; Sigma), and nebulin (N9891; Sigma) was quantified. The maximum number of nonoverlapping images was obtained at 20× magnification. An investigator blinded to mouse genotype used ImageJ 1.46r to determine the optical density of the immunofluorescence signal. The threshold was determined by evaluating secondary-only control images, and the optical density was calculated as the product of mean gray value and percent area of signal.

Western Blot Analysis. Protein expression and α-DG glycosylation were analyzed in whole homogenate EDL muscle preparations (61). Samples were resolved on SDS/PAGE 3–12% gradient gels before transfer to PVDF membranes, visualized by Western blotting, and quantified using the Li-cor Odyssey Infrared Imaging System.

Statistical Analyses. Values are expressed as means ± 1 SE. All listed sample sizes represent the number of analyzed samples, with each sample originating from a distinct mouse (i.e., sample size represents biological replicates rather than technical replicates). Comparisons between two groups were performed using Student's *t* test whereas data consisting of more groups were analyzed using ANOVA. When normality or equal variance could not be assumed, data were analyzed using the Mann–Whitney Rank Sum test or Kruskal–Wallis analysis of variance on ranks. All post hoc pairwise multiple comparisons were done using the Student–Newman–Keuls Method. $P < 0.05$ was considered statistically significant.

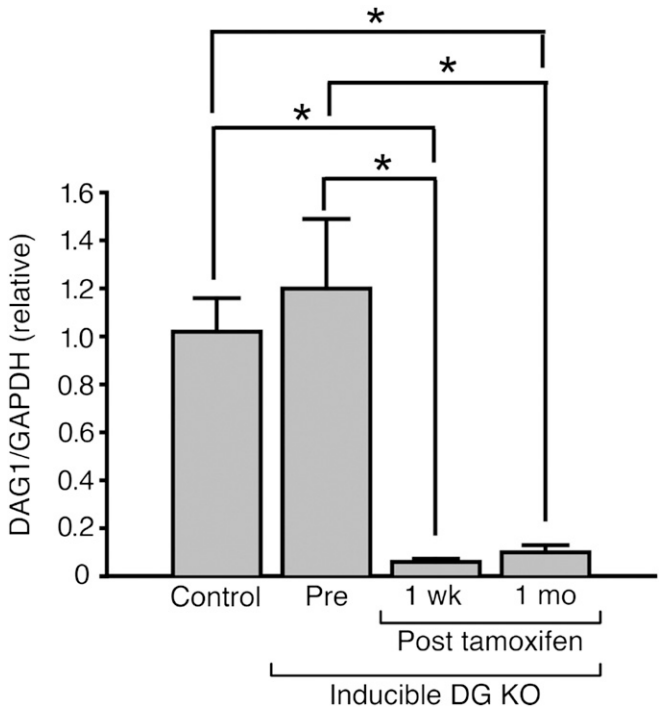

Fig. S1. *Dag1* mRNA levels decrease rapidly in muscles of inducible DG KO mice after exposure to tamoxifen. A reduction in *Dag1* mRNA levels was observed for inducible DG KO mice as early as 1 wk post-tamoxifen exposure. $n = 3$ per group. Values are means ± SE; *$P < 0.05$.

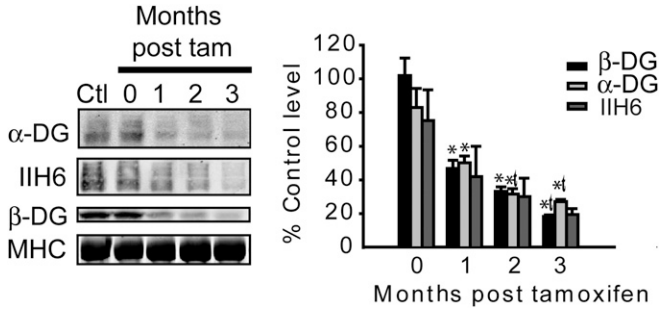

Fig. S2. Progressive reduction in DG expression upon tamoxifen exposure in skeletal muscle of inducible DG KO mice. Similar reductions in protein levels were observed for core α-DG, glyco-α-DG (IIH6), and the C terminus of β-DG as analyzed by Western blot analysis of EDL muscle ($n = 3$–4 per group). (*Left*) Representative Western blot results. (*Right*) Quantification of the Western blot analysis. For IIH6, a trend for decreased protein levels was observed after tamoxifen exposure (ANOVA main effect of time, $P = 0.096$). For core α-DG and β-DG, significance was reached. *, significant difference ($P < 0.05$) from values for the same antibody at 0 mo (i.e., before tamoxifen administration). t, significant difference ($P < 0.05$) from values for the same antibody 1 mo post-tamoxifen exposure. No differences were observed between 2- and 3-mo time points.

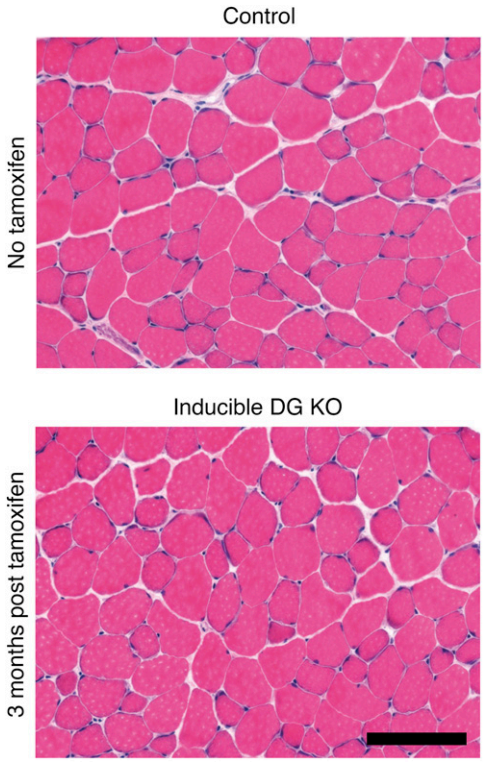

Fig. S3. Absence of overt necrosis observed during the first several months after the induction of reduced DG levels. H&E-stained EDL muscle sections from control mice (i.e., mice that were cre-negative floxed *Dag1*) without exposure to tamoxifen (*Upper*) and inducible DG KO mice at 3 mo post-tamoxifen (*Lower*). (Scale bar: 100 μm.)

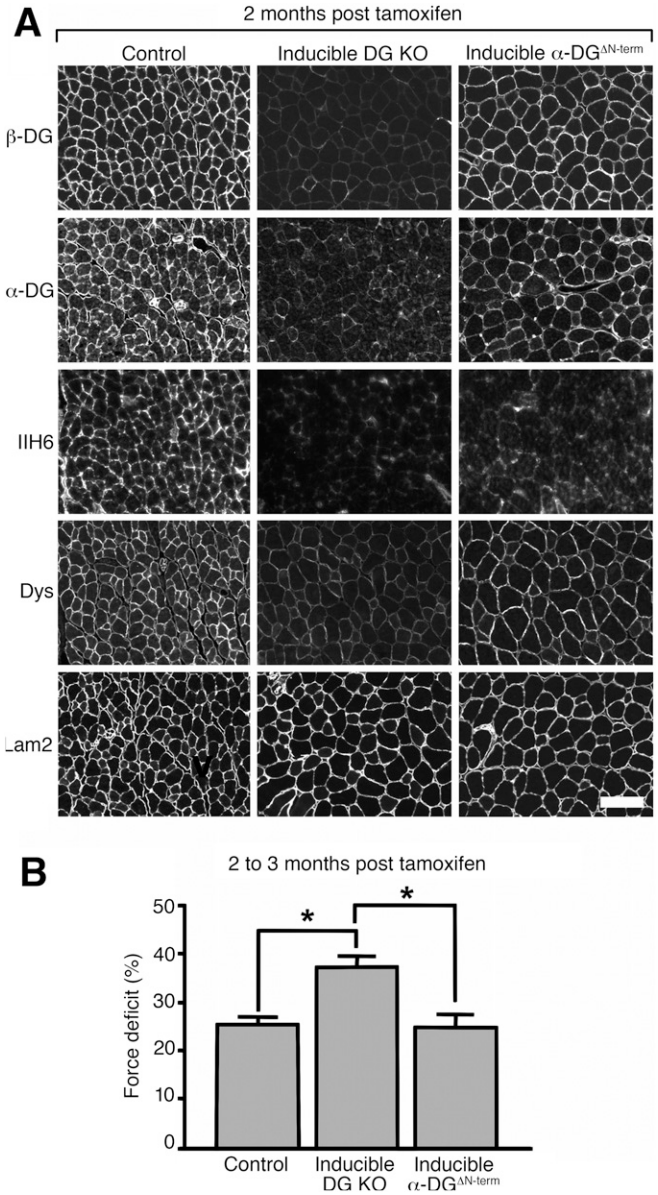

Fig. S4. Susceptibility to contraction-induced injury is not increased when β-DG and core α-DG are maintained at WT levels. Exposure to tamoxifen for inducible α-DG$^{\Delta N\text{-term}}$ mice caused the replacement of fully glycosylated α-DG with α-DG lacking the N-terminal domain. (*A*) Expression of β-DG, α-DG core, IIH6, dystrophin (Dys), and laminin α2 (Lam2) analyzed by immunofluorescence. IIH6 staining was diminished for inducible α-DG$^{\Delta N\text{-term}}$ mice. Less dystrophin staining was observed in the inducible DG KO muscle but not in the inducible α-DG$^{\Delta N\text{-term}}$ muscle. (Scale bar: 100 μm.) (*B*) At 2–3 mo post-tamoxifen, muscles of inducible α-DG$^{\Delta N\text{-term}}$ mice sustained lengthening contraction force deficits at levels similar to control mice (n = 4–5 per group). Values are means ± SE; *$P < 0.05$.

Table S1. Muscle size and measures of isometric force used to determine specific force and force deficit values for control and inducible DG KO mice at 1, 2, and 3 mo post-tamoxifen exposure

Control at 1 mo	
Muscle mass, mg	10.4 ± 0.5
L_o, mm	13.0 ± 0.2
CSA, mm^2	1.7 ± 0.1
Pre-LCP force, mN	409 ± 16
Post-LCP force, mN	288 ± 17
Inducible DG KO at 1 mo	
Muscle mass, mg	10.5 ± 0.1
L_o, mm	12.9 ± 0.4
CSA, mm^2	1.7 ± 0.1
Pre-LCP force, mN	402 ± 38
Post-LCP force, mN	269 ± 24
Control at 2 mo	
Muscle mass, mg	11.5 ± 1.1
L_o, mm	13.5 ± 0.3
CSA, mm^2	1.8 ± 0.2
Pre-LCP force, mN	436 ± 38
Post-LCP force, mN	282 ± 22
Inducible DG KO at 2 mo	
Muscle mass, mg	10.5 ± 0.6
L_o, mm	13.4 ± 0.1
CSA, mm^2	1.6 ± 0.1
Pre-LCP force, mN	389 ± 17
Post-LCP force, mN	223 ± 15
Control at 3 mo	
Muscle mass, mg	11.5 ± 0.9
L_o, mm	13.3 ± 0.2
CSA, mm^2	1.8 ± 0.1
Pre-LCP force, mN	424 ± 14
Post-LCP force, mN	300 ± 21
Inducible DG KO at 3 mo	
Muscle mass, mg	11.2 ± 0.9
L_o, mm	13.2 ± 0.3
CSA, mm^2	1.8 ± 0.1
Pre-LCP force, mN	363 ± 16
Post-LCP force, mN	200 ± 12

Muscle mass, optimal muscle length (L_o), and cross-sectional area (CSA) were assessed, and isometric tetanic forces were measured pre- and post-lengthening contraction protocol (LCP). n = 5–9 per group. Values shown are means ± SE.

Table S2. Measures of isometric force used to determine force deficit, under specific buffer conditions, for muscles of inducible DG KO mice 2–3 mo post-tamoxifen exposure and for *mdx* mice

Mdx: buffer	
Pre-LCP force, mN	361 ± 16
Post-LCP force, mN	210 ± 13
Mdx: buffer + NAC	
Pre-LCP force, mN	260 ± 17
Post-LCP force, mN	203 ± 18
Mdx: buffer − Ca^{2+}	
Pre-LCP force, mN	338 ± 15
Post-LCP force, mN	241 ± 15
Inducible DG KO: buffer	
Pre-LCP force, mN	367 ± 21
Post-LCP force, mN	245 ± 9
Inducible DG KO: buffer + NAC	
Pre-LCP force, mN	356 ± 20
Post-LCP force, mN	246 ± 19
Inducible DG KO: buffer − Ca^{2+}	
Pre-LCP force, mN	384 ± 26
Post-LCP force, mN	240 ± 13

Isometric tetanic force was measured pre- and post-lengthening contraction protocol (LCP). n = 5–9 per group. Values shown are means ± SE.

Table S3. Measures of isometric force used to determine force deficit values in assessing caffeine potentiation for control and inducible DG KO mice at 2–3 mo post-tamoxifen exposure

Control	
Pre-LCP force, mN	431 ± 25
Post-LCP force, mN	300 ± 12
Post-LCP force with caffeine, mN	349 ± 18
Inducible DG KO	
Pre-LCP force, mN	431 ± 37
Post-LCP force, mN	233 ± 25
Post-LCP force with caffeine, mN	278 ± 33

Isometric tetanic forces were measured pre- and post-lengthening contraction protocol (LCP), as well as after exposure to 10 mM caffeine. n = 5 per group. Values shown are means ± SE.

Table S4. Measures of muscle size and passive tension used to determine values of passive tension normalized to cross-sectional area (CSA) for control and inducible DG KO mice at 2–3 mo post-tamoxifen exposure

Control	
Muscle mass, mg	12.5 ± 0.7
L_o, mm	13.8 ± 0.2
CSA, mm^2	1.9 ± 0.1
Pre-LCP passive tension, mN	81 ± 7
Post-LCP passive tension, mN	57 ± 4
Inducible DG KO	
Muscle mass, mg	12.3 ± 0.7
L_o, mm	13.6 ± 0.1
CSA, mm^2	1.9 ± 0.1
Pre-LCP passive tension, mN	98 ± 7
Post-LCP passive tension, mN	54 ± 3

Muscle mass, optimal muscle length (L_o), and CSA were assessed, and passive tension was measured pre- and post-lengthening contraction protocol (LCP). n = 8 per group. Values shown are means ± SE.

Table S5. Optical density values (a.u.) of immunofluorescence signals for various cytoskeletal/sarcomeric proteins in muscles at rest or after LCP, from mice 2–3 mo post-tamoxifen exposure

Protein and mice	Rest	LCP
Nebulin		
Control	22.4 ± 0.5	20.3 ± 3.8
Inducible DG KO	25.3 ± 5.1	25.3 ± 5.7
Desmin		
Control	57.6 ± 4.4	50.3 ± 3.1
Inducible DG KO	54.0 ± 2.7	53.6 ± 3.2
α-Actinin		
Control	42.1 ± 2.5	51.6 ± 4.6
Inducible DG KO	44.8 ± 6.8	44.8 ± 4.6

Values shown are means ± SE. $n = 3$ per group. No significant differences were observed between muscles at rest and after LCP conditions.

Table S6. Muscle size and measures of isometric force used to determine specific force and force deficit values for control, inducible DG KO, and inducible $DG^{\Delta N\text{-term}}$ mice 2–3 mo post-tamoxifen exposure

Control	
Muscle mass, mg	11.9 ± 1.0
L_o, mm	14.1 ± 0.2
CSA, mm^2	1.8 ± 0.1
Pre-LCP force, mN	471 ± 24
Post-LCP force, mN	350 ± 12
Inducible DG KO	
Muscle mass, mg	13.1 ± 0.9
L_o, mm	14.2 ± 0.2
CSA, mm^2	1.9 ± 0.1
Pre-LCP force, mN	426 ± 14
Post-LCP force, mN	268 ± 15
Inducible α-$DG^{\Delta N\text{-term}}$	
Muscle mass, mg	11.4 ± 1.2
L_o, mm	14.0 ± 0.2
CSA, mm^2	1.7 ± 0.2
Pre-LCP force, mN	411 ± 28
Post-LCP force, mN	294 ± 17

Muscle mass, optimal muscle length (L_o), and cross-sectional area (CSA) were assessed, and isometric tetanic forces were measured pre- and post-lengthening contraction protocol (LCP). $n = 4–5$ per group. Values shown are means ± SE.